

## Effects of Long-Chain Acyl-Coenzyme A's on the Activity of the Soluble Form of Nicotinamide Adenine Dinucleotide Phosphate-Specific Isocitrate Dehydrogenase from Lactating Bovine Mammary Gland<sup>1</sup>

Harold M. Farrell, Jr.,\*<sup>2</sup> Edward D. Wickham,\* and Henry C. Reeves†

\*Agricultural Research Service, United States Department of Agriculture, Eastern Regional Research Center, 600 East Mermaid Lane, Philadelphia, Pennsylvania 19118; and †Department of Microbiology, Arizona State University, Tempe, Arizona 85287

Received March 3, 1995, and in revised form May 19, 1995

The cytosolic form of NADP<sup>+</sup>:isocitrate dehydrogenase, a primary source of the NADPH required for *de novo* fatty acid synthesis in lactating bovine mammary gland, was studied to determine possible mechanisms of regulation by fatty acyl-coenzyme A (CoA). The reduction of NADP<sup>+</sup> by the enzyme is inhibited by palmitoyl-CoA. In steady-state experiments, when added enzyme is used to start the reaction, analyses of velocity versus palmitoyl-CoA concentration as a binding isotherm, following the assumptions of Wyman's theory of thermodynamic linkage, suggested that binding of palmitoyl-CoA produced two different inhibitory effects on the enzyme. This analysis suggested inhibition first through binding to sites with an average dissociation constant of 3.3  $\mu\text{M}$ , then by binding to sites with an average dissociation constant of 294  $\mu\text{M}$ . When the enzyme is preincubated with palmitoyl-CoA there is an induction of a significant lag-burst reaction rate (hysteretic kinetics). Preincubation of the enzyme with its substrate, metal-isocitrate complex, nearly abolished the lag time and decreased the degree of inhibition. Changes in lag time and percentage inhibition as a function of concentration of palmitoyl-CoA followed patterns, similar to those observed in steady-state reactions, where the enzyme is not preincubated. Examination of the effect of acyl chain length at 300  $\mu\text{M}$  demonstrated that only long-chain CoA's with carbon numbers >14 have pronounced effects on kinetics. CoA alone has little or no effect, while stearoyl-CoA

completely inhibited the enzyme. Other C<sub>18</sub> acyl groups produced varying effects depending on the degree of unsaturation and *cis-trans* isomerism. NADP<sup>+</sup>:Isocitrate dehydrogenases, from other sources including that from *Escherichia coli*, do not show such sensitivity to acyl chain character under these conditions. Concentration ranges observed for these transitions are compatible with physiological conditions. This suggests that complexes of acyl-CoA's and NADP<sup>+</sup>:isocitrate dehydrogenase, in tissue rich in the cytoplasmic form of the enzyme, could be related to cytoplasmic events in the synthesis and secretion of lipid and possibly protein, since palmitoyl-CoA is known to promote secretory processes through acylation reactions which lead to vesicle fusion.

Academic Press, Inc.

The enzyme, NADP<sup>+</sup>-dependent isocitrate dehydrogenase (IDH)<sup>3</sup> [*threo*-D<sub>5</sub>-isocitrate:NADP<sup>+</sup> oxidoreductase (decarboxylating), EC 1.1.1.42], can serve as source of NADPH for synthesis of metabolic end products in a variety of tissues such as adrenal gland, kidney, and liver (1, 2). In lactating ruminant mammary gland, this enzyme may be a primary source of the NADPH required for fatty acid and cholesterol synthesis (3, 4). A survey of the distribution of Krebs cycle enzymes in bovine mammary tissue showed that NADP<sup>+</sup>:IDH is predominately cytosolic (>90%) in nature and that little or no NAD<sup>+</sup>:IDH activity is present

<sup>1</sup> Mention of brand or firm names does not constitute an endorsement by the U.S. Department of Agriculture over others of a similar nature not mentioned.

<sup>2</sup> To whom correspondence should be addressed. Fax: 215-233-6559.

<sup>3</sup> Abbreviations used: IDH, isocitrate dehydrogenase; MS, metal-isocitrate complex; CoA, coenzyme A; G-6-PDH, glucose-6-phosphate dehydrogenase.

(5). The latter enzyme is known to be allosterically regulated by metabolites and is thought to be a major point of control of Krebs cycle activity (6, 7); its absence in bovine mammary gland raises the question as to what might control this important step in mammary Krebs cycle activity. Previous reports from this laboratory have dealt with the effects of substrates, cofactors, and inhibitors on the modulation of cytosolic IDH activity (8, 9). However, a recent report of the inhibition of the mitochondrial dehydrogenases by fatty acyl-CoA derivatives (10) raised the question as to whether such inhibition could occur for the soluble form of IDH, since Plaut *et al.* (11) have demonstrated immunologic and electrophoretic differences for the cytosolic and mitochondrial forms of mammalian IDH. An intriguing feature of lactating mammary gland, a lipogenic tissue, is the occurrence of long-chain CoA's in the cytoplasm (3), so investigations of the kinetic properties of the cytosolic enzyme and the effects of CoA derivatives on its structure and activity were undertaken to gain further insight into possible mechanisms which may regulate this enzyme in lactating bovine mammary gland.

## EXPERIMENTAL PROCEDURES

**Materials.** All coenzymes, substrates, and biochemicals (including pig heart NADP<sup>+</sup>:isocitrate, and glutamic dehydrogenases) used in this study were purchased from either Sigma Chemical Co. (St. Louis, MO) or Calbiochem (San Diego, CA). Blue Sepharose CL-6B and Sephacryl S-200 were products of Pharmacia (Piscataway, NJ), and DE-32 was obtained from Whatman (Clifton, NJ). All other chemicals were reagent grade.

Whole mammary glands from cows of known good health and productivity were obtained through the cooperation of J. E. Keys of USDA (Beltsville, MD). The whole mammary glands were obtained at the time of slaughter, trimmed to remove adipose tissue, and sectioned into pieces approximately  $10 \times 15 \times 5$  cm. The tissue was frozen on dry ice and stored at  $-80^{\circ}\text{C}$  until used. NADP<sup>+</sup>:IDH was purified to homogeneity as described by Farrell (12). NADP<sup>+</sup>:Isocitrate dehydrogenase from *Escherichia coli* was purified as previously described (13).

**Enzyme assays.** NADP<sup>+</sup>:Isocitrate dehydrogenase activity was measured at a constant temperature of  $25^{\circ}\text{C}$  by monitoring the increase in absorbance at 340 nm. The standard reaction mixture consisted of 100 mM tris (hydroxymethyl) aminomethane hydrochloride salt (Tris · HCl) at pH 7.4, 0.330 mM MnSO<sub>4</sub>, 3.00 mM D,L-isocitrate, and 110 μM NADP<sup>+</sup> in a total volume of 1.00 ml; 10 μl of enzyme was added to start the reaction. For the *E. coli* enzyme the only change was to increase the concentration of NADP<sup>+</sup> to 200 μM to be more in line with the reported  $K_m$  (13). Throughout this study, only Mn<sup>2+</sup> was used; therefore, "metal" will be used to refer to Mn<sup>2+</sup>, although Mg<sup>2+</sup> can replace it with only minor effects (12). Concentrations of metal-citrate, metal-isocitrate, and free metal ion were computed as previously described (14). One enzyme unit catalyzes the formation of 1.0 μmol/min of NADPH at  $25^{\circ}\text{C}$ . Specific activity is defined as enzyme units per milligram of protein.

**Data analysis of enzyme kinetics.** Nonlinear regression analyses of progress curves and variance of other parameters with concentration were carried out using the program Abacus, which is based on the Gauss-Newton iterative method and which was developed by William Damert (Eastern Regional Research Center). Choices between fits of models and statistical methods of analysis of the nonlin-

ear fits were as described by Meites (15). In each case, the iterative analysis was carried out until a minimum value for the root mean square was found. The data were tested by *F* test for improved fit at each change in the integer values (15).

**Estimation of the critical micelle concentration of palmitoyl-CoA.** The critical micelle concentration of palmitoyl-CoA was estimated by using Ultrafree PF-membrane filter units (Millipore/Continental Water Systems, Bedford, MA) containing polysulfone membranes with a nominal cutoff of 30,000 molecular weight. The total concentration of palmitoyl-CoA was estimated from the starting solution (1 ml) and the samples were filtered under pressure at  $25^{\circ}\text{C}$  in a constant temperature box. Samples containing varying amounts of total acyl-CoA were filtered and the nonmicellar concentration was taken to be that of the filtrate. The retentate was assumed to be the micellar fraction and its concentration was estimated by subtracting the concentration of the filtrate from total. The buffer system was identical to the standard incubation assays but without NADP<sup>+</sup> or enzyme. In these experiments the free Mn<sup>2+</sup> concentration is set at 80 μM by the preselected concentrations of metal and isocitrate. Analysis of the polymer vs monomer curves at fixed free metal gave an estimated critical micelle concentration of  $35 \pm 3$  μM for three experiments.

## RESULTS

**Effect of palmitoyl-CoA on NADP<sup>+</sup>:IDH.** Using the standard assay conditions developed for the soluble form of IDH (12), slight inhibition by palmitoyl-CoA (~10%) was observed. The palmitoyl-CoA concentration was 100 μM, and enzyme was added to start the reaction. Since palmitoyl-CoA is somewhat structurally homologous to the phosphoadenosine portion of NADP<sup>+</sup>, it could act as a weak competitive inhibitor of cofactor binding. The effects of 10, 100, and 300 μM palmitoyl-CoA on the initial velocity of the enzyme as a function of NADP<sup>+</sup> concentration were studied. In the absence of palmitoyl-CoA,  $K_m$  for NADP<sup>+</sup> was found to be 12 μM, in agreement with previously reported values (12). At 10 μM, palmitoyl-CoA appears to be a competitive inhibitor of NADP<sup>+</sup> (Fig. 1b). However, at 100 μM palmitoyl-CoA (Fig. 1c), the fitted line diverges. At 300 μM (Fig. 1d),  $V_{max}$  also appears to be effected, and the parallel nature of the lines suggests noncompetitive inhibition. To further test the effects of palmitoyl-CoA, a greater range of concentrations was used at a constant NADP<sup>+</sup> concentration of 110 μM ( $10 \times K_m$ ). The reaction rate drops sharply at first, then levels off and falls again, indicative of biphasic behavior (Fig. 2a).

The traditional analysis of the Dixon plot ( $1/v$  vs  $I$ ) suppresses the sensitivity of the best data found at lowest  $[I]$  but by the use of nonlinear regression analysis, data can be directly fitted without the need for mathematical transformations or weighting factors. Following the concepts developed by Wyman (16) and used in our laboratory for linked-function analysis of the effects of ligand binding (17), a change in the observed velocity of an enzyme by substrate or an inhibitor is most likely thermodynamically linked to binding (8) to the enzyme. As previously shown for IDH (8) it may be assumed (for example, Fig. 2a) that for an en-

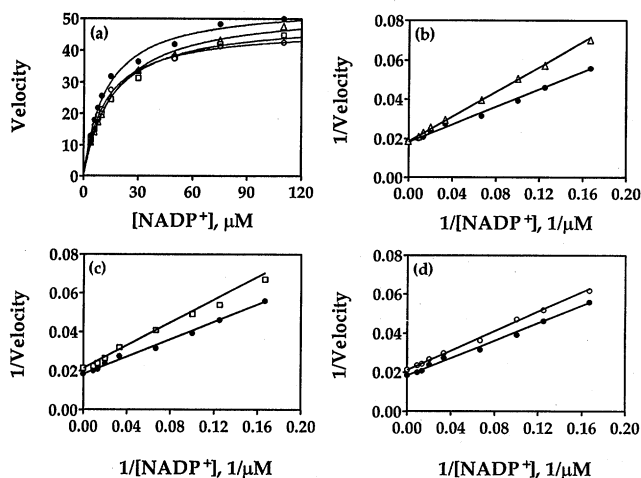


**FIG. 1.** Effect of concentration of palmitoyl-CoA on the variation of the reaction rate of NADP<sup>+</sup>:IDH from lactating bovine mammary gland with NADP<sup>+</sup>. The experiments were carried out in triplicate under standard reaction conditions; the concentrations of palmitoyl-CoA used were 10, 100, and 300 μM. Data were fitted directly to velocity (μmol per minute per milligram of protein) vs [S] data by nonlinear regression analysis of the standard Michaelis equation in (a) (●, control; Δ, 10 μM; □, 100 μM; ○, 300 μM). The theoretical double reciprocal lines from the calculated constants were then plotted and reactions in the presence of palmitoyl-CoA compared with control values (●). Comparisons are 10 μM (Δ) in (b), 100 μM (□) in (c), and 300 μM (○) in (d).

zyme ( $E$ ), whose final velocity ( $V_f$ ) is affected by an inhibitor ( $I$ ) in two different ways, the following equilibria exist for the enzyme:

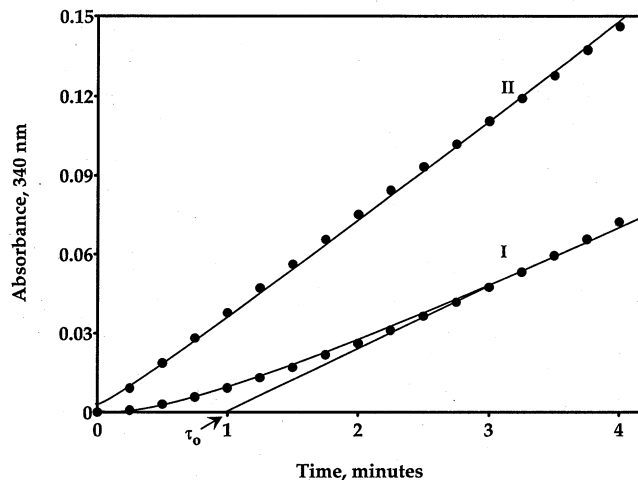
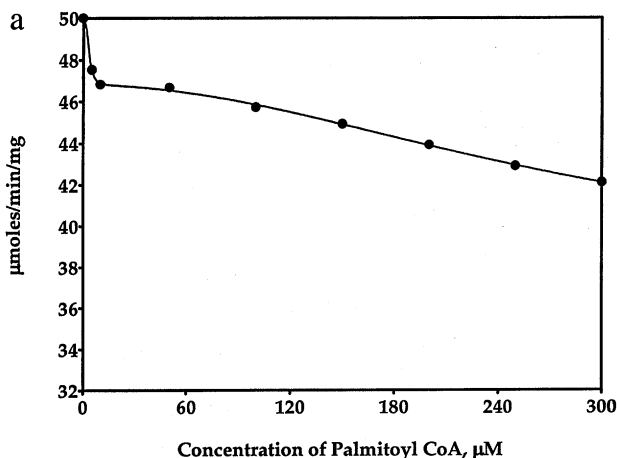
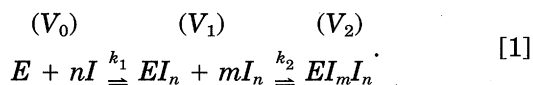


**FIG. 3.** Time course of the reaction of NADP<sup>+</sup>:isocitrate dehydrogenase. The enzyme was incubated under two conditions. Curve I: enzyme incubated with palmitoyl-CoA. The final linear portion can be thought of as  $V_f$ ; the intercept of this line at  $A_{340} = 0$  is the lag time  $\tau_0$  and its reciprocal is  $k$ . Curve II: enzyme preincubated with metal substrate and no palmitoyl-CoA. In each case the solid line shown is the actual fit to Eq. [5]; the concentrations after mixing are those of standard assay and the palmitoyl-CoA is 300 μM.

Preliminary analyses of Fig. 2a indicated two responses of  $V_f$  to palmitoyl-CoA. The simplest mathematical description of this observation yielding the best fit to the data is

$$V_{\text{obs}} = V_0 f_E + V_1 (f_{EI_n} - f_{EI_n I_m}) + V_2 f_{EI_n I_m} \quad [2]$$

where  $V_0$  is the apparent maximum velocity ( $V_{\text{max}}$ ) in the absence of concentration-dependent binding of an

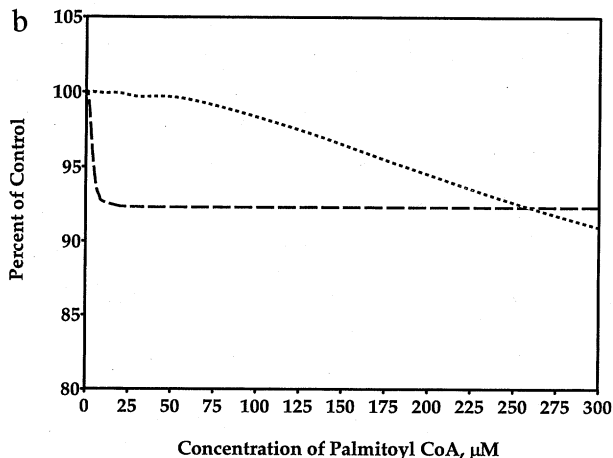


**FIG. 2.** (a) Plot of velocity at  $V_{\text{max}}$  conditions (μmol per minute per milligram of protein) for IDH against the concentration of palmitoyl-CoA; the concentration of free  $\text{Mn}^{2+}$  was fixed at 80 μM and that of  $\text{Mn}^{2+}$ -isocitrate at 250 μM; variations of palmitoyl-CoA were then calculated. Reactions were started by addition of enzyme, and each point was run in triplicate. Data were fitted with Eq. [3] using the assumptions of thermodynamic linkage of velocity to binding of  $I$  (palmitoyl-CoA). (b) Simulation of the inhibition of the IDH by the two classes of sites suggested by analysis of (a). The fitted parameters for each site are given in Table I and the simulation is in percentage of control. — —, Site 1; ---, Site 2.

TABLE I

Parameters Obtained for Linked-Function Analysis of the Variation of Isocitrate Dehydrogenase Velocity,  $V_{\max}$ , with Palmitoyl-CoA<sup>a</sup> Concentration

State <sup>b</sup>	Exponents <sup>c</sup>	$K_D \pm SD^d$ ( $\mu\text{M}$ )	$V_i^e$ ( $\mu\text{mol}/\text{min}/\text{mg}$ )
$V_0$	—	—	$50.1 \pm 0.1$
$V_1$	3	$3.3 \pm 0.25$	$46.8 \pm 0.1$
$V_2$	2	$294 \pm 26$	$37.5 \pm 0.8$

<sup>a</sup> Calculated values and error of coefficients of  $K_D$  and  $V_i$ , each point in triplicate; total error of the fit was 2%. Data of Fig. 2a were fitted as previously described (8).

<sup>b</sup> State of the enzyme  $\pm I$  as previously defined (8).

<sup>c</sup> Integer exponents  $n$  and  $m$  as previously defined (8).

<sup>d</sup> Calculated dissociation constant ( $1/k$ ), with standard error of estimate.

<sup>e</sup>  $V_i$  represents the predicted theoretical  $V$  (with standard error) contributed by each state and produced by the binding of each class of palmitoyl-CoA as previously described;  $V_0$  represents calculated  $V_{\max}$  in the absence of palmitoyl-CoA.

effector molecule ( $I$ ), and  $V_1$  and  $V_2$  represent velocities contributed by each state represented in the stoichiometric Eq. [1] as modulated by the fraction ( $f$ ) of enzyme in each state. The analysis presupposes that  $k_1 > k_2$  and that  $k_1$  and  $k_2$  represent binding to noninteracting classes of independent sites. Other models were tested, including two cooperative sites and one independent site, but the fits were poor and not justified statistically (15). Following the method of Wyman (16), thermodynamic linkage of the binding of  $I$  to change in velocity can be derived by substituting terms for binding of  $I$  into Eq. [2] and assuming total enzyme concentration to be constant as previously described (8). For data following the behavior seen in Fig. 2a, the equation is

$$V_{\text{obs}} = \frac{V_0}{1 + k_1^n I^n} + V_1 \left[ \frac{k_1^n I^n}{1 + k_1^n I^n} - \frac{k_2^m I^m}{(1 + k_2^m I^m)} \right] \quad [3]$$

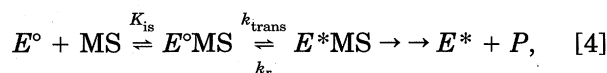
$$+ \frac{V_2 k_2^m I^m}{(1 + k_2^m I^m)}$$

Here the association constants ( $k_i$ ) and the terms  $n$  and  $m$  have the meanings expressed in the stoichiometric Eq. [1]. Because Michaelis–Menten conditions are employed,  $[I]$  is taken to be the total concentration of  $I$  fixed at the beginning of the experiment. The data were fitted by nonlinear regression analysis using integer values for  $n$  and  $m$ ; Eq. [3] implies no interaction between the two classes of sites.

Statistical analysis (15) of the data shown in Fig. 2a with a variety of binding isotherms suggested the best curve to be composed of two distinct functions. The results of this analysis, using Eq. [3], are given in Table I. The nonlinear analysis yields numbers for  $k_i$  that,

when viewed in terms of dissociation constants, can be related to physiological concentrations and allows assessment of the relative contributions of  $V_i$  to  $V_{\text{obs}}$ . The averages of these constants are given in Table I. Apparently binding to two different classes of sites may yield two different mechanisms of inhibition in accord with the data of Fig. 1.

*Effect of palmitoyl-CoA on the time course of the IDH reaction.* Previous studies on the kinetics of NADP<sup>+</sup>:IDH from lactating mammary gland showed that the enzyme displayed nonlinear (hysteretic) kinetics of the lag–burst type when examined by stopped-flow techniques (8). In the determination of the Michaelis constants (12) particularly at low metal ion concentrations, early nonlinear portions of the initial velocity curves were observed in standard kinetics experiments. In preliminary experiments designed to test the concentration-dependent effect of palmitoyl-CoA on IDH activity it was noted that when IDH was preincubated for 2 min at 25°C with palmitoyl-CoA (at concentrations of the acyl-CoA  $>100 \mu\text{M}$ ) the enzyme kinetics began to exhibit a very distinct lag time. The reaction coordinate (Fig. 3, curve I) appeared to fit the lag–burst kinetics observed in stopped-flow experiments, where the apparent lag time for the enzyme was calculated to be 5 s (8). In the present experiments preincubation with palmitoyl-CoA increased the apparent lag time to minutes (Fig. 3, curve I). According to one of the theories for hysteretic enzymes (enzymes with nonlinear kinetics) as developed by Frieden (18), the enzyme can be considered to occur in two states, an initial ( $E^\circ$ ) and a final ( $E^*$ ) state; substrate binding facilitates the transition between these states. The best fit found in the stopped-flow work (8) was obtained with a model in which the bound substrate (in the case of IDH, the true substrate is a 1:1 complex of metal and isocitrate (8, 12)) causes the conversion of  $E^\circ\text{MS}$ , which is inactive, to  $E^*\text{MS}$ , which is fully active. For this model, the general scheme given by Frieden (18) was simplified to



where  $E^\circ$  is inactive enzyme,  $E^*$  is active enzyme, MS is metal–isocitrate complex,  $K_{\text{is}}$  is the dissociation constant for  $E^\circ\text{MS}$ ,  $k_{\text{trans}}$  is the rate constant for the conversion of  $E^\circ\text{MS}$  to  $E^*\text{MS}$ , and  $k_r$  is the reverse rate constant for  $E^*\text{MS}$  to  $E^\circ\text{MS}$ .

The integrated form of the equation for appearance of product  $P$  was derived (8) and is

$$P_{\text{obs}} = V_f t - V_f \left( \frac{1 - e^{-kt}}{k} \right), \quad [5]$$

TABLE II  
Effects of Various Preincubation Conditions on the Lag Time ( $\tau$ ) and the Percentage Inhibition<sup>a</sup>

Components first incubation <sup>b</sup>	Components second incubation <sup>b</sup>	$\tau \pm \text{SD}^c$ (s)	$V_f \pm \text{SD}^c$ (%)
Enzyme alone	None	8.2 $\pm$ 5.5	100.0
+MS	None	7.4 $\pm$ 6.3	100.4 $\pm$ 0.5
+PCoA	None	66.5 $\pm$ 5.7	68.0 $\pm$ 2.5
+PCoA	+MS	60.7 $\pm$ 7.0	71.6 $\pm$ 3.4
+MS	+PCoA	13.8 $\pm$ 4.9	88.3 $\pm$ 1.4
+MS + PCoA	None	48.6 $\pm$ 4.5	85.7 $\pm$ 4.7
+NADP <sup>+</sup>	None	9.7 $\pm$ 5.9	99.0 $\pm$ 0.6
+NADP <sup>+</sup>	+PCoA	114 $\pm$ 21	88.3 $\pm$ 1.9
+NADP <sup>+</sup> + PCoA	None	252 $\pm$ 25	107 $\pm$ 2.3

<sup>a</sup> Average of three determinations on each of three enzyme preparations using fits to Eq. [5]. Here the lag time,  $\tau$ , is defined as  $1/k_{\text{obs}}$ ; the final velocity,  $V_f$ , is reported as percentage of control.

<sup>b</sup> Standard reaction concentrations: the concentration of metal-substrate (MS) complex after mixing was fixed at 250  $\mu\text{M}$ , and the free  $\text{Mn}^{2+}$  concentration was fixed at 80  $\mu\text{M}$ . The total metal ( $\text{M}_T^{2+}$ ) was 0.330 mM, and the total substrate ( $S_T$ ) was 3.00 mM. The preincubation time was 2 min at ambient temperature. The total concentration of palmitoyl-CoA (PCoA) was 300  $\mu\text{M}$ . Incubation volumes were 80 to 90% of final; the enzyme was always incubated in the presence of buffers.

<sup>c</sup> Average value  $\pm$  SD for the average of three preparations which therefore represents the between-preparation variation. The error within a preparation was 3 to 5%.

where  $P_{\text{obs}}$  is concentration of observed product,  $V_f$  is velocity of NADP reduction by the enzyme in state  $E^*$ ,  $k$  is rate constant for conversion of  $E^*\text{MS}$  to  $E^*\text{MS}$  ( $k_{\text{trans}}$  of Eq. [4]), and  $t$  is time. Kinetic experiments on NADP<sup>+</sup>:IDH were conducted with preincubation of palmitoyl-CoA at selected concentrations ranging from 2 to 300  $\mu\text{M}$ . Each progress curve was analyzed by nonlinear regression techniques and fitted to various models (8). When the data were fitted with Eq. [5], excellent root mean squares were obtained, and the confidence levels for the fits were all in excess of 95%. Figure 3, curve I shows an example of the actual fit of data to Eq. [5]. This analysis also uses all data points obtained as contrasted with graphical estimates (19) which require an arbitrary choice for the line drawn and which ignore the actual data obtained at early times; an example of graphical analysis is when  $\tau$ , the lag time, and its reciprocal, the transition rate ( $k$ ), are computed as shown in Fig. 3, curve I.

Having established the applicability of Eq. [5], the effects of various preincubation concentrations with and without palmitoyl-CoA can be placed on a quantitative basis by solving for  $k$  (which in each experiment is the value calculated from Eq. [5]) and  $V_f$ , the final value for the reaction rate. The results of a series of preincubation experiments are given in Table II. Preincubation of IDH at 25°C for 2 min in the absence of

acyl-CoA causes the appearance of a lag time. This has been previously observed for enzyme diluted into buffers in the absence of protectants (20). Preincubation with palmitoyl-CoA dramatically increases the calculated lag times from 8 to 67 s and yields over 30% inhibition (Table II). Preincubation with metal-substrate and then with palmitoyl-CoA partially overcomes both effects. When the enzyme is preincubated with palmitoyl-CoA, neither coincubation with metal-substrate nor a following incubation with metal-substrate can appreciably change the lag time and inhibition. Curiously, preincubation with NADP<sup>+</sup> and palmitoyl-CoA actually yields the greatest lag time (Table II). Thus, reaction of IDH with metal substrate precludes the effect of palmitoyl-CoA on lag time only when the IDH and substrate are preincubated for 2 min. Regardless of the effect on lag time,  $V_f$ , the final velocity, is lowered by the palmitoyl-CoA, indicating enzymatic inhibition (Table II) except when the lag time is greatest (IDH, palmitoyl-CoA, and NADP<sup>+</sup> all preincubated).

*Effect of the concentration of palmitoyl-CoA on derived parameters of the enzyme time course.* When the effect of preincubation of IDH with palmitoyl-CoA was studied as a function of acyl-CoA concentration, a biphasic reaction was observed for the calculated value  $V_f$ . The results of a typical experiment are shown in Fig. 4a. A sharp drop in  $V_f$  is seen as the concentration of acyl-CoA is raised, then a second portion occurs in the curve with a more gradual slope. Since the observed lag time also increases as a function of the concentration of palmitoyl-CoA, the lag time was also plotted as a function of acyl-CoA (Fig. 4b). In this instance the first inflection occurs at lower values, but again a second inflection is observed. This curve was also analyzed with Eq. [3], substituting  $\tau_{\text{obs}}$  for  $V_{\text{obs}}$ ; the results are given in Table IV. It can be seen by inspection that the constants here are similar to those observed for the effects on  $V_f$  (compare Tables III and IV). Apparently both classes of sites induce a lag time and have the potential for effects on  $V_f$ , but effects on  $\tau$  are more pronounced on a percentage basis at elevated concentrations of palmitoyl-CoA. (Compare percentage decreased  $V_f$  vs percentage increase in  $\tau$ .) Both sets of derived dissociation constants compare well with those  $k$ 's obtained without preincubation (Table I).

*Effects of CoA and its fatty acyl derivatives on derived parameters.* Preincubation of IDH with unesterified CoA produced essentially no effects on enzyme activity. Little or no lag time was observed over controls and the degree of inhibition was less than 2% even at 300  $\mu\text{M}$ . The effect of palmitate alone could not be accurately tested because of a lack of solubility in the metal ion-containing assay system.

When the degree of inhibition of  $V_f$  and lag time were

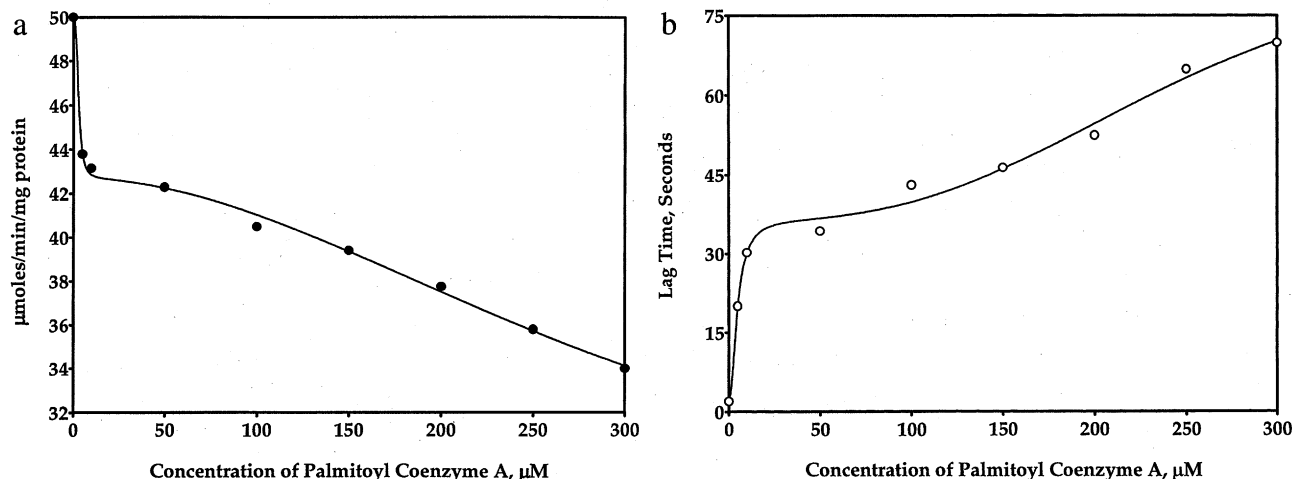


**FIG. 4.** (a) Calculated final velocity ( $V_f$ ) plot under  $V_{max}$  conditions ( $\mu\text{mol}$  per minute per milligram of protein) against the concentration of palmitoyl-CoA; the concentration of free  $\text{Mn}^{2+}$  was fixed at  $80 \mu\text{M}$  and that of  $\text{Mn}^{2+}$ -isocitrate at  $250 \mu\text{M}$ ; variations of palmitoyl-CoA were then calculated. Each point was run in triplicate. Data were fitted with Eq. [3] using the assumptions of thermodynamic linkage of velocity to binding of  $I$  (palmitoyl-CoA). The fitted parameters for each state are given in Table III and averaged for three complete runs. (b) Plot of the variation of the lag time  $\tau$  in seconds against the concentration of palmitoyl-CoA; analysis was as noted for (a) and the derived constants are given in Table IV.

studied as a function of acyl chain length (Figs. 5a and 5b), it was observed that only the longer chain acyl groups significantly affect  $V_f$ . There is an apparent influence of chain length, degree of unsaturation, and *cis-trans* isomer on both  $V_f$  and the lag time. The lag time, however, is not affected until the chain length reaches  $C_{12}$ ; note that  $C_{18:0}$  completely inhibits the enzyme so the lag time is actually infinity. The concentration dependency of the stearoyl-CoA effect is somewhat similar to that of palmitoyl-CoA, except that complete inactivation is observed at  $300 \mu\text{M}$ . This suggests a

possible detergency effect of the CoA derivatives. However, when  $\beta$ -D-octyl thioglucoside was used at the same concentrations as palmitoyl and octyl-CoA's, no effect was found; even at concentrations five times those of the CoA derivatives, no inhibition was observed. This indicates that the effect is not one of a general detergent. Membrane ultrafiltration studies were carried out, as described under Materials and Methods, and yielded a value of  $35 \mu\text{M}$  for the critical micelle concentration of palmitoyl-CoA in the assay system. Finally, differences between stearoyl-CoA,

**TABLE III**

Parameters Obtained for Linked Function Analysis of the Variation of  $V_f$  with Palmitoyl-CoA<sup>a</sup>

State <sup>b</sup>	Exponents <sup>c</sup>	$K_D \pm \text{SD}^d$ ( $\mu\text{M}$ )	$V_i^e \pm \text{SD}$ ( $\mu\text{mol}/\text{min}/\text{mg}$ )
$V_0$	—	—	$50.0 \pm 0.1$
$V_1$	3	$3.73 \pm 0.76$	$44.6 \pm 1.2$
$V_2$	2	$311 \pm 35$	$24.0 \pm 5.0$

<sup>a</sup> Average values and error of coefficients for three complete experiments with three preparations, each point in triplicate; total error of each individual fit averaged 4%. Data of Fig. 4a were fitted with Eq. [3].

<sup>b</sup> State of the enzyme  $\pm I$  as defined in Eq. [1].

<sup>c</sup> Integer exponents  $n$  and  $m$  of Eq. [3].

<sup>d</sup> Calculated dissociation constant ( $1/k$ ), with standard deviation.

<sup>e</sup>  $V_i$  represents the predicted theoretical  $V$  (with standard error of estimate) contributed by each state and produced by the binding of each class of palmitoyl-CoA as described in Eq. [1];  $V_0$  represents calculated  $V_{max}$  in the absence of palmitoyl-CoA.

**TABLE IV**

Parameters Obtained for Linked Function Analysis of the Variation of  $\tau$  with Palmitoyl-CoA<sup>a</sup>

State <sup>b</sup>	Exponents <sup>c</sup>	$K_D \pm \text{SD}^d$ ( $\mu\text{M}$ )	$\tau^e \pm \text{SD}$ (s)
$\tau_0$	—	—	$1.3 \pm 1.0$
$\tau_1$	2/3	$6.1 \pm 1.6$	$21.7 \pm 14.3$
$\tau_2$	3/6	$264 \pm 14.0$	$91.4 \pm 12.6$

<sup>a</sup> Average values and error of coefficients for three complete experiments with three preparations, each point in triplicate; total error of each individual fit averaged 4%. Data of Fig. 4b were fitted with Eq. [3].

<sup>b</sup> State of the enzyme  $\pm I$  as defined in Eq. [1] except  $\tau_i$  replaces  $V_i$ .

<sup>c</sup> Integer exponents  $n$  and  $m$  of Eq. [3].

<sup>d</sup> Calculated dissociation constant ( $1/k$ ), with standard deviation.

<sup>e</sup>  $\tau_i$  represents the predicted theoretical lag time (with standard deviation) contributed by each state and produced by the binding of each class of palmitoyl-CoA as described in Eq. [1];  $\tau_0$  represents calculated  $\tau$  in the absence of palmitoyl-CoA.

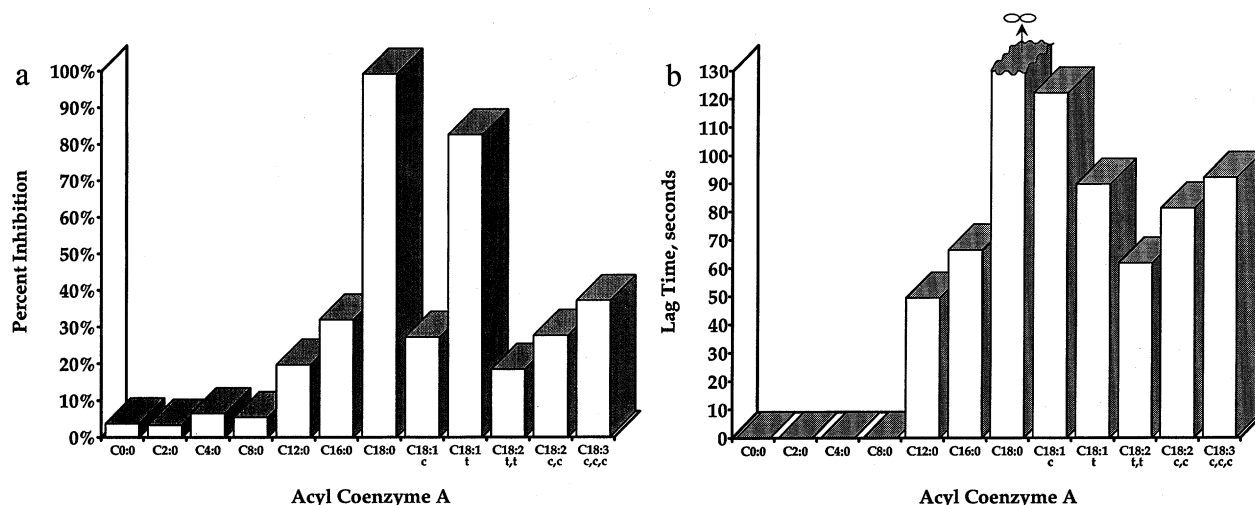


**FIG. 5.** Effect of chain length on the lag time and final velocities of NADP<sup>+</sup>:IDH when preincubated with acyl-CoA's. Each point was run in triplicate and repeated with two other preparations of the enzyme. Conditions are as follows: free Mn<sup>2+</sup>, 80 μM; Mn<sup>2+</sup>-isocitrate, 250 μM; acyl-CoA, 300 μM; Tris buffer, 100 mM, pH 7.4 and 25°C. (a) Bar graph of percentage inhibition calculated from Eq. [5]. (b) Bar graph for τ calculated from Eq. [5].

which is completely inhibitory, and oleoyl-CoA suggest that chain length and/or lipid isomer play a role in inhibition for the soluble form of IDH.

*Effect of palmitoyl-CoA on other types of dehydrogenases.* Previous reports (10) of the effect of palmitoyl-CoA on mammalian dehydrogenases have centered primarily on those of mitochondrial origin. The earliest report however was the inhibition of glucose-6-phosphate dehydrogenase (G-6-PDH) from yeast (21). Having observed the effect of palmitoyl-CoA on the soluble IDH, other enzymes were tested. Preliminary experi-

ments with yeast G-6-PDH confirmed for this assay system the results reported in Ref. 21 (Table V). G-6-PDH from rat mammary cytosol was also completely inhibited with an  $I_{50}$  of 2 μM, but NAD<sup>+</sup>:malate from bovine mammary cytosol was only partially inhibited (~10%) at 300 μM. Glutamic dehydrogenase from bovine liver was inhibited 100% with an  $I_{50}$  of 8 μM whether NAD<sup>+</sup> or NADP<sup>+</sup> were used as cofactors. For these three enzymes, reaction progress curves were essentially linear and exhibited no change upon preincubation with palmitoyl-CoA.

**TABLE V**  
Effects of Palmitoyl-CoA on Selected Dehydrogenases

Enzyme	Tissue source	Lag time, s	Inhibition, %	$I_{50}$ , μM
NADP <sup>+</sup> :IDH	Bovine mammary <sup>a</sup>	60 to 200	10 to 30	4 and 311
	Pig heart (m) <sup>b</sup>	Yes <sup>b</sup>	100	ND <sup>c</sup>
	<i>E. coli</i> <sup>a</sup>	No	100	15
G-6-PDH	Rat mammary (c) <sup>d</sup>	No	100	2.0
	Yeast <sup>e</sup>	NR <sup>f</sup>	100	0.6
Glutamic DH	Bovine liver <sup>g</sup>	No	100	8.0
	NAD <sup>+</sup> :Malate	Bovine mammary (c) <sup>h</sup>	No	10

<sup>a</sup> This study, purified enzymes.

<sup>b</sup> This study, pig heart, commercial enzyme, mitochondrial (m); lag time for lauroyl-CoA only.

<sup>c</sup> ND, not determined.

<sup>d</sup> This study, rat mammary cytosol (c).

<sup>e</sup> Ref. 21 and this study with commercial enzyme.

<sup>f</sup> Not reported in Ref. 21; not observed in this study.

<sup>g</sup> Commercial enzyme with NAD<sup>+</sup> or NADP<sup>+</sup>.

<sup>h</sup> This study, bovine mammary cytosol (c).

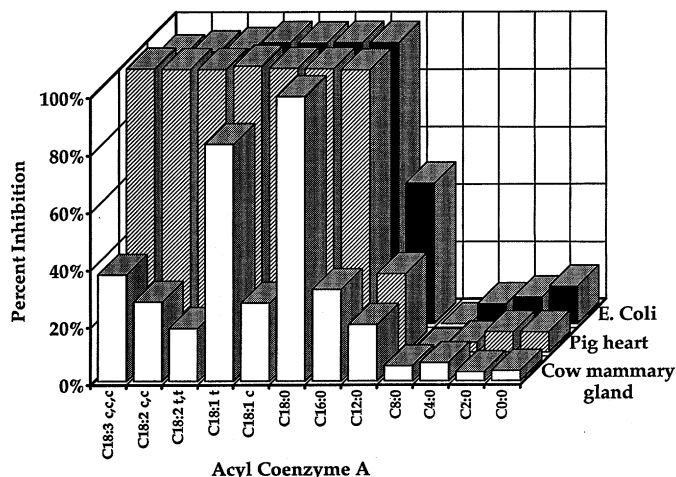


**FIG. 6.** Effect of chain length and *cis-trans* isomerism on the final velocities of NADP<sup>+</sup>:IDH from bovine mammary (open), pig heart (hatched), and *E. coli* (solid) resulting from preincubation of the enzyme with acyl-CoA derivatives. Conditions as given in the legend to Fig. 5.

The comparison to this point has been for eukaryotic systems. The effects of various CoA derivatives on the activity of the *E. coli* IDH were tested by preincubation at 300  $\mu$ M. In this system the *E. coli* IDH gave no hint of nonlinearity for the reaction progress curves. Palmitoyl-CoA completely inhibited the *E. coli* enzyme as did stearoyl-CoA (Fig. 6). When tested at 40  $\mu$ M, where inhibition is partial, no lag times were observed. The concentration dependence of the inhibition of the *E. coli* enzyme also differed, displaying only one class of sites with a  $K_I$  of 15  $\mu$ M (Table V). As an extension of Fig. 5, various C<sub>18</sub> derivatives were tested. The mammary IDH responds dramatically to chain conformation for C<sub>18</sub> acids, while the *E. coli* enzyme does not at 300  $\mu$ M. Interestingly, the *E. coli* enzyme is also affected by C<sub>12</sub>, whereas the mammary IDH is not.

The eukaryote isozyme of IDH, localized in mitochondria, is typified by the pig heart enzyme (1). With respect to acyl-CoA inhibition, the pig heart (mitochondrial) IDH (Fig. 6) is more like the *E. coli* enzyme in that there does not appear to be any variation in inhibition with changes in acyl-CoA chain length and/or *cis-trans* isomers for those  $\geq$ C<sub>16</sub>. This is clearly a difference between cytosolic IDH and the mammalian mitochondrial and *E. coli* forms. With respect to lag time, the pig heart enzyme does exhibit lag time but only with C<sub>12</sub> and, as noted above, is completely inhibited by C<sub>16</sub> acyl-CoA. In mammalian cytoplasm the normal end product of fat synthesis is C<sub>16</sub>, while chains of C<sub>18</sub> and above usually represent dietary intake; this differential response to chain lengths of CoA derivatives may be cytoplasmic specific in lipogenic mammalian systems.

## DISCUSSION

The apparent lack of NAD<sup>+</sup>:IDH in bovine mammary gland (5) has led to the speculation that the activity of the soluble form of NADP<sup>+</sup>:IDH might be influenced by metabolites and, thus, in some way serve a regulatory function in this tissue and perhaps elsewhere. Work carried out on heart (mitochondrial) NADP<sup>+</sup>:IDH (19) had shown nonlinear kinetics under stopped-flow conditions, indicating a lag-burst hysteretic mechanism as delineated by Frieden (18). Similar results for mammary (soluble) NADP<sup>+</sup>:IDH have also been reported (8). The latter workers developed a computer method for calculation of the magnitude of the lag time and its dependence on substrate concentration (8) as well as the effect of inhibition on the progress curves. In the current study, unique fits of these progress curves were also obtained directly by nonlinear regression analysis with Eq. [5]. This analysis allows for calculation of the observed rate constant,  $k$ , for the transition from inactive to active form under a variety of conditions (e.g., Table II). The lag times observed here in the presence of palmitoyl-CoA are significantly greater than those produced by absence of MS in the stopped-flow experiments (8).

Recent studies of the effect of long-chain acyl-CoA's on dehydrogenases have been centered on the role of these molecules in possible regulation and control of brain mitochondrial dehydrogenases such as  $\alpha$ -ketoglutarate, glutamic, and isocitrate dehydrogenases (10). In these latter studies, inhibition of NADP<sup>+</sup>:IDH by palmitoyl-CoA was observed at elevated concentrations (1 mM), but the reaction progress curves were not reported. Lai and Cooper (10) theorized that the CoA derivatives could function to dampen the flux through the Krebs cycle in brain mitochondria. Introduction of a lag time in the enzyme reaction could effectively do this regardless of whether the enzyme is mitochondrial or cytosolic in nature. Substrate level-mediated lag times are of the order of 5 s for cytoplasmic IDH (8). Here the palmitoyl-CoA increases the lag time observed *in vitro* to 60 s for preincubated enzyme and to 252 s for the competitive assay where both CoA derivative and cofactor are preincubated simultaneously (Table II).

For mammary IDH two classes of acyl-CoA binding sites appear to influence activity. There is good agreement in apparent  $K_D$  values regardless of whether the parameter followed is initial velocity, final velocity, or lag time. The overall result is one class of sites at  $\sim$ 3  $\mu$ M and one at  $\sim$ 300  $\mu$ M. Citrate synthase, whose activity is regulated by acyl-CoA derivatives as well (22), also appears to have two classes of sites for these compounds. For citrate synthase, two distinct noninteracting binding sites were demonstrated by spin-labeling methods; they occur at 35 and 98  $\mu$ M and represent

two potential mechanisms of inhibition by fatty acyl-CoA derivatives. In a related study, Powell and co-workers (23) showed that the critical micelle concentration for selected fatty acyl-CoA compounds in buffers ranged from 30 to 60  $\mu\text{M}$ , ruling out the concept of a general detergent effect for the first class of sites for citrate synthase. These workers suggested selective binding as the mechanism of inhibition for this class. Powell *et al.* also observed no correlation between critical micelle concentrations of acyl-CoA derivatives and degree of inhibition of citrate synthase (23), and since the spin labels (22) showed two classes of binding sites, the conclusion was reached that formation of a micelle is not the direct cause of inhibition at the second class of sites of citrate synthase. Membrane ultrafiltration experiments of palmitoyl-CoA in the IDH buffer system with no enzyme present estimated the critical micelle concentration to be 35  $\mu\text{M}$ , in line with the data of Powell *et al.* (23). Thus, micellization is most likely not the cause of the inhibition observed for IDH for the first class of sites and most likely not for the second class either.

The effect of acyl chain length on mammary IDH is unique. The short-chain acyl-CoA's which are typical of milk lipids have no apparent effect; however, palmitoyl-CoA, the major end product of *de novo* mammary lipid synthesis, produces a modest effect. Stearoyl-CoA, which is primarily dietary for ruminants and not an end product of metabolism, completely inhibits the enzyme. The additional two  $\text{CH}_2$  groups appear to dramatically influence access to the active site. Oleoyl-CoA with a *cis* double bond does not effectively prevent NADPH formation and in fact this CoA is similar to palmitoyl-CoA in its effects. Interestingly, bovine mammary gland does contain a desaturase enzyme which can convert stearoyl- to oleoyl-CoA (24). It has been speculated that this desaturase may somehow control lipid synthesis (24, 25). If indeed the desaturase can modify cytosolic stearoyl-CoA, then the desaturase enzyme could indirectly modulate NADPH production through control of the oleoyl/stearoyl ratio which in milk is about 3.5 to 1 (3). The  $\text{C}_{18:1}$  *trans* isomer (another dietary acid) acts like  $\text{C}_{18:0}$  and inhibits the enzyme completely.

In contrast, *E. coli* IDH is inhibited completely by all  $\text{C}_{18}$  fatty acyl-CoA's. This is of particular interest because the crystal structure of the *E. coli* IDH is known (26). The phosphoadenosine binding site is in a cleft above the active site. The fatty acyl chain could prevent substrate binding by interacting with hydrophobic groups such as tyrosine 160 of *E. coli* occurring near the substrate site. If a homologous structure exists for mammary enzyme, this could explain why preincubation with substrate can alleviate inhibition, resulting from decreased interactions between the acyl chain and the tyrosine. This hypothesis is sup-

ported by the fact that the active site of  $\text{NADP}^+:\text{IDH}$  from mammary gland does show a perturbation in the tyrosine CD spectra on binding in the MS complex (9) and the sequences centering on tyrosine 160 of *E. coli* are preserved in yeast, pig heart, and rat ovary enzymes (27). A significant difference does occur between the *E. coli* and eukaryotic IDH's in that the regulatory serine phosphate found in the *E. coli* enzyme is apparently absent (27) in eukaryotes.

In nonruminant species the concentration of  $\text{NADP}^+:\text{IDH}$  is quite low in lactating mammary gland (3, 5). In rat and other monogastric animals, mammary gland G-6-PDH and 6-phosphogluconate dehydrogenase are the primary sources of reducing equivalents for *de novo* lipid synthesis. As reported for the yeast enzyme (21), the cytosolic G-6-PDH of rat mammary gland is strongly inhibited by palmitoyl-CoA at 10  $\mu\text{M}$ . In this study we found that bovine liver glutamic dehydrogenase was completely inhibited at 100  $\mu\text{M}$  palmitoyl-CoA and no lag times were introduced for either G-6-PDH or glutamic dehydrogenase. The other major dehydrogenase found in mammary cytosol ( $\text{NAD}^+:\text{malate}$ ) was almost unaffected by palmitoyl-CoA. Thus, each enzyme tested has relatively unique responses to the acyl-CoA derivatives. This is probably related to the proximity of the  $\text{NAD(P)}^+$  sites to the substrate binding sites of the respective enzymes.

In all species of mammals studied to date, the lactating mammary gland produces milk through two separate ultrastructural pathways (3, 28). Lipid secretion is distinct from skim milk secretion which proceeds through Golgi vesicles released from the secretory cells by reverse pinocytosis. Based upon the data of Baldwin and Yang (29), the apparent total CoA concentration in lactating bovine mammary gland can be estimated to be 200  $\mu\text{M}$ . Stearate, palmitate, and oleate represent 11, 25, and 35% of the total fatty acid content of milk triglycerides; thus, the approximate total concentration of these acyl-CoA's in mammary tissue (transiently) may be as great as 140  $\mu\text{M}$ . Since the concentration of soluble IDH can be estimated to be nearly 50  $\mu\text{M}$  in bovine mammary tissue (5, 12), during the time of net lipid synthesis a substantial portion of cytosolic acyl-CoA could be bound to IDH with a moderate  $K_D$  of 3.3  $\mu\text{M}$ . The potential role of soluble  $\text{NADP}^+:\text{IDH}$  in ruminant tissues could be twofold: first, providing NADPH for synthesis and, second, binding (and possibly transporting) the product of synthesis, fatty acyl-CoA's. The experiments presented here are by nature *in vitro*, but the transitions occur well within the physiological range of many lipogenic tissues. Recent research on modulation of intracellular calcium in pancreatic  $\beta$ -cells pointed to the possibility that >95% of the 90  $\mu\text{M}$  fatty acyl-CoA may be bound to unspecified cytosolic proteins (30); perhaps IDH could be one of these.

## CONCLUSIONS

The importance of enzyme-substrate interactions in the regulation of enzymes has long been recognized (18), as have the principles of allosteric regulation (6, 7). The more recent focus on regulation through metal ion-activated cascades has emphasized the importance of regulatory binding sites with  $K_D \sim 10^{-9}$  (31). The data reported here point to the potential significance of weaker binding sites as regulators of enzyme activity, because metabolite concentrations in mammary tissue occur in the same range as the derived dissociation constants. The effects of palmitoyl-CoA on the enzyme are noteworthy, if the pools of Krebs cycle metabolites in mammary tissue oscillate in the same fashion (1 to 5 s) as the glycolytic pools have been shown to do in other tissues (32); under these circumstances, the long lag times observed in this study could be relevant. While G-6-PDH is completely inhibited at low concentration of palmitoyl-CoA, the soluble NADP<sup>+</sup>:IDH is only partially controlled by this metabolite but is completely inhibited by stearoyl-CoA. Regulation of lipid synthesis could also be achieved through desaturase which could alter the oleoyl/stearoyl-CoA ratio. In addition, it may be speculated that because of the relatively high concentration of NADP<sup>+</sup>:IDH in ruminant tissue it may bind a significant percentage of palmitoyl-CoA, thus limiting (or facilitating) its ability to serve as a cofactor in vesicle fusion (33) which is related to protein secretion. Conversely, the enzyme could limit (or facilitate) transport of the CoA to the nascent droplets for incorporation into triglyceride.

## REFERENCES

1. Colman, R. F. (1983) in *Peptide and Protein Reviews* (Hearn, M. T. W., Ed.), Vol. 1, pp. 41-69, Dekker, New York, NY.
2. Greville, G. D. (1969) in *Citric Acid Cycle: Control and Compartmentation* (Lowenstein, J. M., Ed.), pp. 1-136, Dekker, New York, NY.
3. Bauman, D. E., and Davis, C. L. (1974) in *Lactation* (Larson, B. L., and Smith, V. E., Eds.), Vol. 2, pp. 31-75, Academic Press, New York, NY.
4. Moore, J. H., and Christie, W. W. (1981) in *Lipid Metabolism in Ruminant Animals* (Christie, W. W., Ed.), pp. 227-278, Pergamon Press, Elmsford, NY.
5. Farrell, H. M., Jr., Deeney, J. T., Tubbs, K., and Walsh, R. A. (1987) *J. Dairy Sci.* **70**, 781-788.
6. Chen, R. F., and Plaut, G. W. E. (1963) *Biochemistry* **2**, 1023-1032.
7. Gabriel, J. L., and Plaut, G. W. E. (1984) *J. Biol. Chem.* **259**, 1622-1628.
8. Farrell, H. M., Jr., Deeney, J. T., Hild, E. K., and Kumosinski, T. F. (1990) *J. Biol. Chem.* **265**, 17637-17643.
9. Seery, V. L., and Farrell, H. M., Jr. (1990) *J. Biol. Chem.* **265**, 17644-17648.
10. Lai, J. K. C., and Cooper, A. J. L. (1991) *Neurochem. Res.* **16**, 795-803.
11. Plaut, G. W. E., Cook, M., and Aogaichi, T. (1983) *Biochim. Biophys. Acta* **760**, 300-308.
12. Farrell, H. M., Jr. (1980) *Arch. Biochem. Biophys.* **204**, 551-559.
13. Hy, M., and Reeves, H. C. (1976) *Biochim. Biophys. Acta* **445**, 280-285.
14. Szymanski, E. S., and Farrell, H. M., Jr. (1982) *Biochim. Biophys. Acta* **702**, 163-172.
15. Meites, L. (1979) *CRC Crit. Rev. Anal. Chem.* **8**, 1-53.
16. Wyman, G., Jr. (1964) *Adv. Protein Chem.* **19**, 223-285.
17. Farrell, H. M., Jr., Kumosinski, T. F., Pulaski, P., and Thompson, M. P. (1988) *Arch. Biochem. Biophys.* **265**, 146-158.
18. Frieden, C. (1979) *Annu. Rev. Biochem.* **48**, 471-489.
19. Dalziel, K., McFerran, N., Matthews, B., and Reynolds, C. H. (1978) *Biochem. J.* **171**, 743-750.
20. Seery, V. L., and Farrell, H. M., Jr. (1989) *Arch. Biochem. Biophys.* **274**, 453-462.
21. Eger-Neufelt, I., Teinzer, A., Weiss, L., and Wieland, O. (1965) *Biochem. Biophys. Res. Commun.* **19**, 43-48.
22. Hansel, B. C., and Powell, G. L. (1984) *J. Biol. Chem.* **259**, 1423-1430.
23. Powell, G. L., Grothusen, J. R., Zimmerman, J. K., Evans, C. A., and Fish, W. W. (1981) *J. Biol. Chem.* **256**, 12740-12747.
24. Kinsella, J. E. (1972) *Lipids* **7**, 349-355.
25. Timmen, H., and Patton, S. (1988) *Lipids* **23**, 685-689.
26. Hurley, J. H., Dean, A. M., Koshland, D. E., Jr., and Stroud, R. M. (1991) *Biochemistry* **30**, 8671-8677.
27. Jennings, G. T., Sechi, S., Stevenson, P. M., Tuckey, R. C., Parmelec, D., and McAlister-Henn, L. (1994) *J. Biol. Chem.* **269**, 23128-23134.
28. Leung, C. T., Maleeff, B. E., and Farrell, H. M., Jr. (1989) *J. Dairy Sci.* **72**, 2495-2509.
29. Baldwin, R. L., and Yang, Y. T. (1974) in *Lactation, A Comprehensive Treatise* (Larson, B. L., and Smith, V. R., Eds.), Vol. 1, pp. 349-411, Academic Press, New York, NY.
30. Deeney, J. T., Tornheim, K., Korchak, H. M., Prentki, M., and Corkey, B. E. (1992) *J. Biol. Chem.* **267**, 19840-19845.
31. Cheung, W. Y. (1984) *Fed. Proc.* **43**, 2995-2999.
32. Neet, K. E., and Ainslie, G. R., Jr. (1980) *Methods Enzymol.* **64**, 192-226.
33. Pfanner, N., Glick, B. S., Arden, S. R., and Rothman, J. E. (1990) *J. Cell Biol.* **110**, 955-961.